A multi-year observation of nitrous oxide at the Boknis Eck Time-Series Station in the Eckernförde Bay (southwestern Baltic Sea)

Xiao Ma[1], Sinikka T. Lennartz[1,2], and Hermann W. Bange[1]

[1] GEOMAR Helmholtz Centre for Ocean Research Kiel, Düsternbrooker Weg 20, 24105 Kiel, Germany

[2] now at ICBM, University of Oldenburg, Oldenburg, Germany

Correspondence to: Xiao Ma (mxiao@geomar.de)

Abstract. Nitrous oxide (N_2O) is a potent greenhouse gas and it is involved in stratospheric ozone depletion. Its oceanic production is mainly influenced by dissolved nutrient and oxygen (O_2) concentrations in the water column. Here we examined the seasonal and annual variations of dissolved N_2O at the Boknis Eck (BE) Time-Series Station located in Eckernförde Bay (southwestern Baltic Sea). Monthly measurements of N_2O started in July 2005. We found a pronounced seasonal pattern for N_2O with high concentrations (supersaturations) in winter/early spring and low concentrations (undersaturations) in autumn when hypoxic/anoxic conditions prevail. Unusually low N_2O concentrations were observed during October 2016–April 2017, which was presumably a result of prolonged anoxia and the subsequent nutrient deficiency. Unusually high N_2O concentrations were found in November 2017 and this event was linked to the occurrence of upwelling which interrupted N_2O consumption via denitrification and potentially promoted ammonium oxidation (nitrification) at the oxic/anoxic interface. Nutrient concentrations (such as nitrate, nitrite and phosphate) at BE are decreasing since 1980s, but oxygen concentrations in the water column are still decreasing. Our results indicate a close coupling of N_2O anomalies to O_2 concentration, nutrients and stratification. Given the long-term trends of declining nutrient and oxygen concentrations at BE, a decrease in N_2O concentration, and thus emissions, seems likely due to an increasing number of events with low N_2O concentrations.

1. Introduction

Long-term observation with regular measurement intervals can be an effective way to monitor seasonal and interannual variabilities as well as to decipher short- and long-term trends of an ecosystem, which are required to make projections of the future ecosystem development (see e.g. Ducklow et al., 2009). Recently, multi-year time-series measurements of nitrous oxide (N_2O), a potent greenhouse gas and a major threat to ozone depletion (IPCC, 2013; Ravishankara et al., 2009), have been reported from the coastal upwelling areas off central Chile (Farías et al., 2015) and off Goa (Naqvi et al., 2010), in the North Pacific Subtropical Gyre (Wilson et al., 2017), and in Saanich Inlet (Capelle et al., 2018).

N_2O production in the ocean is generally dominated by microbial nitrification ($NH_4^+ \rightarrow NO_2^- \rightarrow NO_3^-$) and denitrification ($NO_3^- \rightarrow NO_2^- \rightarrow N_2O \rightarrow N_2$). During bacterial/archaeal nitrification, N_2O is produced as a by-product with enhanced N_2O production under low oxygen (O_2) conditions (e.g. Goreau et al., 1980; Löscher et al., 2012). N_2O is produced as an intermediate during bacterial denitrification (Codispoti et al., 2005). N_2O could be further consumed via denitrification to dinitrogen, however, this process is inhibited with the presence of O_2 because of the low O_2 tolerance of the enzyme involved (Bonin et al. 1989). This incomplete pathway is called partial denitrification and can lead to N_2O accumulation (e.g. Naqvi et al., 2000; Farías et al., 2009).

The oceans including coastal areas contribute ~25% of the natural and anthropogenic N_2O emissions (IPCC, 2013), with disproportionately high emissions from coastal and estuarine areas (Bange, 2006). N_2O emissions from coastal areas strongly depend on nitrogen inputs (Seitzinger and Kroeze, 1998; Zhang et al., 2010). The increasing input of nitrogen (i.e. eutrophication) has become a worldwide problem in coastal waters leading to enhanced productivity and severe O_2 depletion caused by enhanced degradation of organic matter (Breitburg et al., 2018; Rabalais et al., 2014). The decline in O_2 concentration (i.e. deoxygenation), either in coastal waters or the open ocean, might result in favorable conditions for N_2O production (Codispoti et al., 2001; Nevison et al., 2003). The results of a model study by Kroeze and Seitzinger (1998) indicated a significant increase of N_2O in European coastal waters for 2050. Moreover, it has been suggested that N_2O production and emissions are very likely to increase in the near future, especially in the shallow suboxic/anoxic coastal systems (Naqvi et al., 2000; Bange, 2006). However, model projections show a net decrease in future global oceanic N_2O emission during the 21st century (Martinez-Rey et al., 2015; Landolfi et al., 2017; Battaglia and Joos, 2018).

The Baltic Sea is a nearly enclosed, marginal sea with a very limited access to the open ocean via the North Sea. The restricted water exchange with the North Sea and extensive human activities, such agriculture, industrial production and sewage discharge in the catchment area led to high inputs of nutrients to the Baltic Sea. As a result, the areas affected by anoxia have been expanding in the deep basins of the central Baltic Sea (Carstensen et al., 2014). In order to control this situation, the Helsinki Commission (HELCOM) was established in 1974 and a series of measures have been taken to prevent anthropogenic nutrient input into the Baltic Sea. Consequently, the nutrient inputs (by riverine loads, direct point-sources and, for nitrogen, atmospheric deposition) to the Baltic Sea are declining (HELCOM, 2018a). However, the number of low O_2 (i.e. hypoxic/anoxic) events in coastal waters of the Baltic Sea is increasing and deoxygenation is still going on (Conley et al., 2011; Lennartz et al., 2014). The deoxygenation in the Baltic Sea can affect the production/consumption of N_2O. Our group has been monitoring dissolved N_2O concentrations at the Boknis Eck Time-Series Station, located in Eckernförde Bay (southwestern Baltic Sea), for more than a decade. In this study, we present monthly measurements of N_2O and biogeochemical parameters such as nutrients and O_2 from July 2005 to December 2017. The major objectives of our study were: 1) to decipher the seasonal

pattern of N_2O distribution in the water column, 2) to identify short-term and long-term trends of the N_2O concentrations, 3) to explore the potential role of nutrients and O_2 for N_2O production/consumption, and 4) to quantify the sea–to–air N_2O flux density at the time-series station.

2. Material and methods

2.1 Study site

Sampling at the Boknis Eck (BE) Time-Series Station (www.bokniseck.de) started on 30 April 1957 and, therefore, it is one of the oldest continuously operated time-series stations in the world. The BE station is located at the entrance of the Eckernförde Bay (54°31′ N, 10°02′ E, Fig. 1) in the southwestern Baltic Sea. The water depth of the sampling site is 28 m. Various physical, chemical and biological parameters are measured on a monthly basis (Lennartz et al., 2014). There is no significant river runoff to Eckernförde Bay. Hence, the hydrographical conditions are mainly dominated by saline water input from the North Sea and less saline water from the Baltic Proper, which is typical for that region. Seasonal stratification usually starts to develop in April and lasts until October, during which hypoxia or even anoxia (characterized by the presence of hydrogen sulphide, H_2S) sporadically occurs, as a result of restricted vertical water exchange and bacterial decomposition of organic matter in the bottom water (Hansen et al., 1999; Lennartz et al., 2014). Thus, BE is a natural laboratory to study the influence of O_2 variations and anthropogenic nutrient loads on N_2O production/consumption.

2.2 Sample collection and measurement

Monthly sampling of N_2O at the BE Time-Series Station started in July 2005. Triplicate samples were collected from six depths (1, 5, 10, 15, 20 and 25 m). Seawater was drawn from 5 L Niskin bottles into 20 mL brown glass vials after overflow. The vials were sealed with rubber stoppers and aluminum caps. The bubble-free samples were poisoned with 50 µL of a saturated mercury chloride ($HgCl_2$) solution and then stored in a cool, dark place until measurement. The general storage time before measurements of the N_2O concentrations was less than three months.

The static headspace-equilibrium method was adopted to measure the dissolved N_2O concentrations in the vials. 10 mL helium (99.9999 %, AirLiquide, Düsseldorf, Germany) headspace was created in each vial with a gas-tight glass syringe (VICI Precision Sampling, Baton Rouge, LA). Samples were vibrated with Vortex (G-560E, Scientific Industries Inc., New York, USA) for 20 seconds and then left for at least two hours until equilibrium. 9.5 mL subsample of the headspace was subsequently injected into a GC-ECD (gas chromatograph equipped with the electron capture detector) system (Hewlett-Packard 5890 Series II, Agilent Technologies, Santa Clara, CA, USA), which was calibrated with two standard gas mixtures (N_2O in synthetic air, 320 ppb and 1000 ppb, Deuste-Steininger GmbH, Mühlhausen, Germany and Westfalen AG, Münster, Germany) prior to the measurement. The average precision of the

measurements, calculated as the median standard deviation from triplicate measurements, was 0.4 nM. Triplicates with a standard deviation of >10% were omitted. More details about the N_2O measurement can be found in Kock et al. (2016). Dissolved oxygen (O_2) concentrations were measured by Winkler titrations (Grasshoff et al., 1999). Nutrient concentrations were measured by the Segmented Continuous Flow Analysis (SCFA, Grasshoff et al., 1999). A more detailed summary of the parameters measured and methods applied can be found in Lennartz et al. (2014).

2.3 Times series analysis

A time-series can be decomposed into three main components, i.e. trend, cycle and residual component (Schlittgen and Streitberg, 2001). We used the Mann–Kendall test and wavelet analysis to detect the trend and periodical cycles in the time-series data, respectively. As for the residual component, we highlight unusual high/low N_2O concentrations during 2005-2017 and discuss the potential causes for these events.

2.3.1 Wavelet analysis

In order to decipher periodical cycles of the parameters collected at the BE Time-Series Station, a wavelet analysis method was adopted. Wavelet analysis enables the detection of the period and the temporal occurrence of repeated cycles in time-series data. One of the requirements for wavelet analysis is a regular, continuous time-series. Since there is data missing (maximum 2 months in a row) in the BE time-series, due to terrible weather or the ship's unavailability, missing data was interpolated from the previous and following months. Sampling time varied for every month (usually 20-40 day interval), but for the statistical analysis, data was assumed to be regularly spaced as differences on weekly scales were minor. Considering the band width in both frequency and time domain, a Morlet mother wavelet with a wave number of 6 was chosen (Torrence and Compo, 1998). The mother wavelet was then scaled between the frequency of a half-year cycle and the length of the time-series with a stepsize of 0.25. The wavelet analysis was conducted with the MatLab code by Torrence and Compo [2004]. More information about the method can be found on the website http://paos.colorado.edu/research/wavelets/.

2.3.2 Mann–Kendall test

Mann–Kendall test (MKT) is a non-parametric statistical test to assess the significance of monotonic trends for time-series measurements. It tests the null hypothesis that all variables are randomly distributed against the alternative hypothesis that a monotonic trend, either increase or decrease, exists in the time-series on a given significance level α (here α=0.05). MKT is flexible for data with missing values and the results are not impacted by the magnitude of extreme values, which makes it a widely used test in hydrology and climatology (e.g. Xu et al., 2003; Yang et al., 2004). However, MKT is sensitive to serial correlation in the time-series. The presence of positive serial correlation would increase the probability of trend detection even though no such trend exists (Kulkarni and von Storch, 1995). In order to avoid this situation, data from 12

months were tested individually. It is assumed that there is no residual effect left from the same month last year, considering that the nitrogen species are rapidly biologically cycled. The Matlab function from Simone (2009) was used for the MKT.

2.4 Calculation of saturation and sea–to–air flux density

N_2O saturations (S_{N2O}, %) were calculated as:

$$S_{N2O} = 100 \times N_2O_{obs}/N_2O_{eq} \quad (1)$$

where N_2O_{obs} and N_2O_{eq} (in nM) are the observed and equilibrated N_2O concentrations in seawater, respectively. N_2O_{eq} was computed as a function of surface seawater temperature, in situ salinity (Weiss and Price, 1980) and the dry mole fractions of atmospheric N_2O at the time of the sampling. Since the atmospheric N_2O mole fractions were not measured at the BE Time-Series Station, atmospheric dry mole fractions of N_2O were derived from the monthly average of N_2O data at Mace Head, Ireland (AGAGE, http://agage.mit.edu/), instead.

N_2O flux density (F_{N2O}, in μmol m^{-2} d^{-1}) was calculated as:

$$F_{N2O} = k_{N2O} \times (N_2O_{obs} - N_2O_{eq}) \quad (2)$$

where k_{N2O} (in cm h^{-1}) is the gas transfer velocity calculated with the method given by Nightingale et al. (2000), as a function of the wind speed and the Schmidt number (*Sc*). The wind speed data were obtained from the Kiel Lighthouse (see: www.geomar.de/service/wetter/), which is approximately 20 km away from the BE Time-Series Station. The wind speed was normalized to 10 m (u_{10}) to calculate k_{N2O} (Hsu et al., 1994). k_{N2O} was adjusted by multiplying with $(Sc/600)^{-0.5}$, and *Sc* was computed as:

$$Sc = v/D_{N2O} \quad (3)$$

$$D_{N2O} = 3.16 \times 10^{-6} e^{-18370/RT} \quad (4)$$

where *v* is the kinematic viscosity of seawater, which is calculated from the empirical equations given in Siedler and Peters (1986), and D_{N2O} is the diffusion coefficient of N_2O in seawater. *R* is the universal gas constant and *T* is the water temperature in K.

3. Result and discussion

3.1 Overview

N_2O concentrations at the BE Time-Series Station showed significant temporal and depth-dependent variations from 2005 to 2017 (Fig. 2). N_2O concentrations fluctuated between 1.2 and 37.8 nM, with an overall average of 13.9±4.2 nM. This value was higher than the results from the surface water of Station ALOHA (5.9–7.4 nmol kg^{-1}, average 6.5±0.3 nmol kg^{-1}, Wilson et

al., 2017), which is reasonable considering the weak anthropogenic impact in the North Pacific Subtropical Gyre. The N_2O concentrations at BE were much lower than those measured at the time-series station in the coastal upwelling area off Chile (2.9–492 nM, average 39.4±29.2 nM in the oxyclines and 37.6±23.3 nM in the bottom waters, Farías et al., 2015) and a quasi-time series station off Goa (Naqvi et al., 2010), where significant N_2O accumulations were observed in subsurface waters at both locations. Our measurements were comparable to the time-series station from Saanich Inlet (~0.5–37.4 nM, average 14.7 nM, Capelle et al., 2018), a seasonally anoxic fjord which has similar hydrographic conditions as BE.

NO_2^- concentrations fluctuated between below detection limit of 0.1 μM and 1.6 μM, with an average of 0.2±0.3 μM. NO_3^- concentrations varied from below detection limit of 0.3 μM to 17.9 μM, with an average of 2.0±2.8 μM. The temporal and spatial distributions of nitrite (NO_2^-) and nitrate (NO_3^-) were similar during 2005–2017. A clear O_2 seasonality can be seen with severe O_2 depletion in the bottom waters during summer and autumn. Anoxia with the presence of H_2S were detected in September/October 2005, September 2007, September/October 2014, and September–November 2016. All of the extremely low N_2O concentrations (<5 nM) were observed in the bottom waters in autumn, coinciding with hypoxia/anoxia, while the high N_2O concentrations (>20 nM) sporadically occurred at different depths either in spring or autumn.

3.2 Seasonal cycle

Significant cycles at different frequencies were detected via wavelet analysis at the BE Time-Series Station during 2005–2017 (Fig. 3). A half-year NO_2^- cycle sporadically occurred in 2007–2009, 2013 and 2015. There is a seasonal NO_2^- variability (at the frequency of 1 year) between 2007 and 2016 (times before 2007 and after 2016 were outside the conic line), except during 2010–2012, when high NO_2^- concentrations were not observed in winter (Fig. 2). A biennial cycle of NO_2^- could be observed as well during 2008–2015. The NO_3^- concentrations were dominated by an annual cycle and a minor half-year cycle. The biennial cycle only occurred in 2008 and 2009. A remarkable seasonal variability of dissolved O_2 prevailed all the time, which is also obvious from the times series data shown in Fig. 2. The annual N_2O cycle became gradually more and more evident until 2014, then declined and reoccurred less intensely in 2016. The periodical cycle was also present at other frequencies, indicated by the broadening of the red area before 2015 in Fig. 2d. For example, a biennial N_2O cycle occurred during 2013–2015.

The half-year cycles of NO_2^- and NO_3^- were probably associated with algae blooms which usually occur in each spring and autumn (Fig. S1 and S2). Since the time between the two blooms differed between years, the cycles were weak and thus not present in every year. Due to the fact that there was no half-year O_2 cycle at all, nutrients apart from O_2 might be the “drivers” of the sporadic half-year N_2O cycle in 2008 and 2015, because N_2O production depends on the concentration of the bioavailable nitrogen compounds (Codispoti et al., 2001).

Generally the wavelet analysis indicated a strong annual cycle for NO_2^-, NO_3^-, dissolved O_2 and N_2O at the BE Time-Series Station, which enabled us to explore the seasonal pattern with annual mean data. Although extreme values were excluded as a result of averaging, the smoothed results generally reflect the seasonality of these parameters. Here, we focus on the annual cycle.

The annual mean vertical distribution of dissolved O_2, NO_2^-, NO_3^- and N_2O are shown in Fig. 4. Due to the development of stratification, the mixed layer was shallow in summer and deep in late autumn/winter. O_2 depletion was observed in bottom waters from late spring until late autumn. The seasonal variations of NO_2^- and NO_3^- were significantly correlated with each other ($[NO_3^-]=11.59[NO_2^-]-0.51$, $R^2=0.80$, $n=72$, $p<0.0001$) and high concentrations were observed for both in winter. Minimum N_2O concentrations were found in the bottom waters during September and October, presumably as a result of consumption during denitrification under anoxic condition (Codispoti et al., 2005). High N_2O concentrations were observed in late spring and late autumn, respectively. In late spring N_2O accumulated in the bottom waters because the stratification prevented mixing of the water column. In late autumn, however, N_2O could be ventilated to the surface and thus emitted to the atmosphere due to the breakdown of the stratification. The high N_2O concentrations could be attributed to enhanced N_2O production via nitrification and/or denitrification within the oxic/anoxic interface (Goreau et al., 1980; Codispoti et al., 1992). Since there is no clear O_2 concentration threshold, N_2O production from both nitrification and the onset of denitrification overlap at oxic/anoxic inteface. To this end, direct N_2O production measurements (i.e. nitrification/denitrification rates) are required to decipher which process dominates the formation of the different N_2O maxima.

High N_2O concentrations prevailed all over the water column in winter/early spring. NH_4^+ is released from the sediment into bottom waters due to the degradation of organic matter, especially after the autumn algae bloom (Fig. S1 and S2). The stratification usually completely breaks down at this time of the year and the water column becomes oxygenated. Denitrification is inhibited by the presence of high concentrations of dissolved O_2 (> 20 μmol L^{-1}) and thus nitrification is presumably responsible for the high N_2O concentrations in winter/early spring.

3.3 Trend analysis

The MKTs were conducted for the surface (1m) and bottom (25m) N_2O concentrations and saturations of the individual 12 months, respectively. Significant decreasing trends were detected for the concentrations in the bottom waters for February and August (Table 1a), and for the saturations in the surface for September and in the bottom for August and November (Table 1b). These results indicated that some systematical changes in N_2O took place at BE. For example, the significant decrease in N_2O concentration/saturation in August might be associated with the increasing temperature, which reinforces the stratification and accelerates O_2 consumption in the bottom waters (Lennartz et al., 2014). As a result, hypoxia/anoxia starts earlier and thus enables the onset of denitrification to consume N_2O. During most of the months, trends in N_2O concentration and saturation were not significant during 2005–2017.

A significant nutrient decline has been observed at the BE Time-Series Station since the mid-1980s, however, Lennartz et al. (2014) found that bottom O_2 concentrations were still decreasing over the past 60 years. The ongoing oxygen decline was attributed to the temperature-enhanced O_2 consumption in the bottom water (Meier et al., 2018) and a prolongation of the stratification period at the BE Time-Series Station (Lennartz et al., 2014). Please note that the trends in nutrients and O_2 concentrations were detected based on the data collection which lasted for approximately 30 and 60 years, respectively, while the N_2O observations at BE Time-Series Station has lasted for only 12.5 years. Further MKT analysis for nutrients, temperature and oxygen for months with significant trends in N_2O concentrations did not show any significant results ($p>0.05$). The significant trends in N_2O concentrations thus do not seem to be directly related to one of these parameters, and we cannot state a reason for the significant trends of N_2O concentration in February and the N_2O saturation in September and November at this point. Presumably, a longer monitoring period for N_2O is required to detect corresponding trends in N_2O and oxygen or nutrients.

3.4 Extreme events

3.4.1 Low N_2O concentrations during October 2016-April 2017

Besides the low N_2O concentrations occurring in autumn, we observed a band of pronounced low N_2O concentrations which started in October 2016 and lasted until April 2017 (Fig. 5). In this period N_2O concentrations varied between 5.5–13.9 nM, with an average of 8.4±2.0 nM. This is approximately 40% lower than the average N_2O concentration during the entire measurement period 2005–2017. The average N_2O saturation during 2005–2017 was 111±30%, while from October 2016 to April 2017, the N_2O saturations were as low as 43–93% (average 62±10%).

Undersaturated N_2O waters have been previously reported from the Baltic Sea: Rönner (1983) observed a N_2O surface saturation of 79% in the central Baltic Sea and attributed the undersaturation to upwelling of N_2O-depleted waters. Bange et al. (1998) found a minimum N_2O saturation of 91% in the southern Baltic Sea where the hydrographic conditions were significantly influenced by riverine runoff. Walter et al. (2006) reported a mean N_2O saturation of 79±11% for shallow stations (<30 m) in the southwestern Baltic Sea in October 2003. The low-N_2O event at BE was unusual because the concentrations were much lower than those reported values and it lasted for more than half a year.

Although the observed temperatures and salinities during October 2016–April 2017 were comparable to other years (Fig. S1), it is difficult to evaluate the role of physical mechanism in the low-N_2O event because of insufficient data for water mass exchange at the BE Time-Series Station. Here we mainly focused on the chemical or biological processes. Anoxia events with the presence of H_2S were observed in the bottom waters for three months in a row during September–November 2016. This is an unusual long period and is unprecedented at the BE

Time-Series Station. In December 2016 the stratification did not completely break down. Although the water column was generally oxygenated, bottom O_2 concentrations were the lowest observed during the past ten years. Considering the classical view of N_2O consumption via denitrification under hypoxic and anoxic conditions, we inferred that denitrification accounted for low N_2O concentrations in the bottom layer. However, the question still remains where the low-N_2O-concentration water in the upper layers came from.

In September 2016, low N_2O concentrations were only observed in the bottom waters where the anoxia occurred. However, the situation was different in the following months. During October/November 2016, N_2O concentrations were homogeneously distributed in the water column. Although the stratification gradually started to break down in late autumn, the density gradient was still strong enough to keep the bottom waters at anoxic conditions and prevented the low-N_2O-concentration to reach the surface. Thus we inferred that the unusual low N_2O concentrations in the upper layers (above 20 m) were probably resulting from advection of adjacent waters. Due to the fact that the upper layers were well-mixed and oxygenated, in situ N_2O consumption in the water column could be neglected. We suggest therefore, that the N_2O depleted waters were resulting from consumption of N_2O in bottom waters elsewhere and then they were upwelled and transported to BE. Hence, N_2O consumption via denitrification might have been, directly or indirectly, responsible for the low N_2O concentrations during October–November 2016.

In December 2016, the bottom waters were ventilated with O_2. Although N_2O consumption by denitrification should have been inhibited by the high concentrations of O_2 (Codispoti et al., 2001), the N_2O concentrations did not restore to their normal level under suboxic conditions. Since January 2017, the whole water column was well mixed and oxygenated. Usually a significant nutrient supply could be observed starting in November (Fig. 4) as a result of remineralization and vertical mixing, but the average NO_2^- and NO_3^- concentrations during November 2016–April 2017 were 0.2 and 1.4 μM, respectively, which was about 50% and 60% lower than in other years. Ammonium (NH_4^+) and chlorophyll *a* concentrations during this period were comparable to that of other years (Fig. S1). Secchi depth, a proxy of water transparency, was 3.8 m in March 2017, which is only slightly lower compared to the monthly average value for March (4.5±1.8 m). There is no exceptional spring algae bloom and thus we infer that assimilative uptake of nutrients by phytoplankton was not responsible for the low nutrients concentrations The nutrient deficiency might be attributed to enhanced nitrogen removal processes like denitrification or anammox (Voss et al., 2005; Hietanen et al., 2007; Hannig et al., 2007) during the prolonged period of anoxia in autumn 2016. During the low N_2O event, we found that N_2O concentrations were positively correlated with both NO_2^- ($[N_2O]=7.02[NO_2^-]+7.36$, $R^2=0.29$, $n=24$, $p<0.01$) and NO_3^- ($[N_2O]=0.80[NO_3^-]+7.36$, $R^2=0.51$, $n=24$, $p<0.0001$). These results indicate that the development and maintenance of the low-N_2O-concentration was closely associated with nutrient deficiency. Especially after the breakdown of

the stratification, when denitrification was no longer a significant N_2O sink, nutrients might have become a limiting factor for N_2O production.

In general, the low-N_2O-concentration event during October 2016–April 2017 can be divided into two parts: in the stratified waters during October–November 2016, O_2 played a dominant role and N_2O was consumed via denitrification under anoxic conditions. In the well-mixed water column during December 2016–April 2017, nutrient deficiency seemed to have constrained N_2O production via nitrification under suboxic/oxic conditions.

In recent years a novel biological N_2O consumption pathway, called N_2O fixation, which transforms N_2O into particulate organic nitrogen via its assimilation, has been reported (Farías et al., 2013). This process can take place under extreme environmental conditions even at very low N_2O concentrations. Cornejo et al. (2015) reported that N_2O fixation might play a major role in the coastal zone off central Chile where seasonally occurring surface N_2O undersaturation was observed. The relatively high N_2 fixation rates in the Baltic Sea (Sohm et al., 2011) highlight the potential role of N_2O fixation (Farías et al., 2013). However, we cannot quantify the role of biological N_2O fixation for the N_2O depletion in the Baltic Sea due to the absence of N_2O assimilation measurements.

3.4.2 High N_2O concentrations in November 2017

High N_2O concentrations were observed at the BE Time-Series Station in November 2017. The average value reached 35.4±1.5 nM, which was the highest concentration measured during the entire sampling period from 2005 to 2017. Dissolved N_2O was homogeneously distributed in the water column, but this event did not last long. In December, dissolved N_2O returned to normal levels and the average concentration in the water column was comparable to that of other years. Average N_2O saturation in November 2017 was 322±10%, which was also the highest for the past 12.5 years. This value was much higher than the maximum surface N_2O saturation reported by Rönner (1983) in the central Baltic Sea, but was comparable to the results observed in the southern Baltic Sea (312%, Bange et al., 1998). Bange et al. (1998) linked the enhanced N_2O concentrations to riverine runoff because those samples were collected in an estuarine area, however, the riverine influence around the BE Time-Series Station is negligible. As a result, the impact of fresh water input can be excluded.

Dissolved O_2 seemed to play a dominant role in the high N_2O concentrations. Enhanced N_2O production usually occurred at the oxic/anoxic interface, which was closely linked to the development of water column stratification. In general the breakdown of the stratification is faster than its establishment at the BE Time-Series Station. As a result, it took about half a year for bottom O_2 saturation to gradually decrease from ~80% to almost 0% (i.e. anoxia), but only two months to restore normal saturation level in 2010 (Fig. 6). In late autumn, surface water penetrated into the deep layers via vertical mixing and eroded the oxic/anoxic interface. The entire water column quickly became oxygenated and the enhanced N_2O production was stopped.

Hypoxia/anoxia at BE is usually observed in the bottom waters in autumn, but in September 2017, hypoxic water (O_2 saturation<20 %, which was close to the criterion for hypoxia, see Naqvi et al., 2010) was found in the subsurface layer (10 m) as well. Surface O_2 saturation was only ~50%, which was the lowest during the sampling period 2005–2017. The density gradient of the water column in September 2017 was much lower than in other years. These results indicate the occurrence of an upwelling event at BE Time-Series Station in autumn 2017, which might be a result of the saline water inflow from the North Sea considering the change of salinity in the water column (Fig. S1). Strong vertical mixing has interrupted the hypoxia/anoxia and bottom O_2 saturation reached ~60% in October 2017. The presence of O_2 prevented N_2O consumption via denitrification, as a result, we did not observe a significant N_2O decline during that period (Fig. 5).

Considering the fact that a significant autumn algae bloom was observed in autumn 2017 (as indicated by high chlorophyll a concentrations, see Fig. S1), severe O_2 depletion in the bottom water could be expected. Although the bottom O_2 saturation was only slightly lower in November than in October, we speculate that even lower O_2 saturation (but not anoxia) might have occurred between October and November. The "W-shaped" O_2 saturation curve (see Fig. 6) suggests that the stratification did not completely break down in October and that there might have been a reestablishment of the oxic/anoxic interface providing favorable conditions for enhanced N_2O production. Due to the degradation of organic nitrogen, NH_4^+ is released from the sediment into bottom waters (Dale et al., 2011), especially in autumn when O_2 is low (Fig. S2). NH_4^+ concentrations in November 2017 were lower than in other years (Fig. S1), and NO_2^- concentrations were higher (Fig. 5), indicating that nitrification occurred in bottom waters. To this end, we suggest that the reestablishment of the oxic/anoxic interface promoted ammonium oxidation (the first step of nitrification). In this case, N_2O could have temporary accumulated because its consumption via denitrification was blocked. Meanwhile, the relatively low density gradient (i.e. low stratification) allowed upward mixing of the excess N_2O to the surface. However, we inferred that that this phenomenon would only last for a few days due to the rapid breakdown of stratification at the BE Time-Series Station.

Due to the development of the pronounced stratification, the oxic/anoxic interface prevailed in summer/early autumn as well, but we did not observe N_2O accumulation during these months. One of the potential explanations is that enhanced N_2O production only took place within particular depths where strong O_2 gradient existed, but our vertical sampling resolution was too low to capture this event. Also enhanced N_2O production might be covered by the weak mixing which brought low-N_2O water from the bottom to the surface.

The upwelling event played different roles in autumn 2016 and 2017. First, upwelling took place somewhere else but at BE because of the strong density and O_2 gradient in the water column during autumn 2016. Second, bottom water remained anoxic in autumn 2016, while the compensated water for upwelling in 2017 penetrated through stratification and brought O_2 into bottom water (Fig. 6), which caused enhanced N_2O production. Similarly, autumn upwelling was

detected in 2011 and 2012 when we found relatively low O_2 concentrations in subsurface layers (10 m) (Fig. 2), but we did not observe an increase in bottom O_2 concentrations and N_2O concentrations remained low during that time. These upwelling events seem to be driven by saline water inflow considering the prominent increase in salinity, but the mechanism dominates O_2 input into bottom water before the stratification break down remains unclear.

3.5 Flux density

During 2005–2017, surface N_2O saturations at the BE Time-Series Station varied from 56 % to 314 % (69–194 % excluding the extreme values discussed in Sect. 3.4), with an average of 111±30 % (111±20 % without the extreme values). Generally the water column at BE was slightly oversaturated with N_2O. Our results are in good agreement with the estimated mean surface N_2O saturation for the European shelf (113%, Bange, 2006).

We found a weak seasonal cycle for surface N_2O concentrations, with high N_2O concentrations occurring in winter/early spring and low concentrations occurring in summer/autumn, but no such cycle for N_2O saturation (Fig. 4; Fig. 7). The seasonality in concentration but not in saturation could be largely attributed to the effect of temperature on N_2O solubility: In summer when surface N_2O concentrations are low, N_2O saturations are increased by the relative high temperature; and vice versa in winter. Although salinity also affects N_2O solubility, its contribution is negligible compared to temperature. Temperature alleviated the fluctuation of surface N_2O saturation and thus affected the sea-to-air N_2O fluxes. We conclude that temperature plays a modulating role for N_2O emissions.

The wind speed (u_{10}) at the BE Time-Series Station ranged from 1.1 to 14.0 m s^{-1}, with an average of 7.0±2.7 m s^{-1}. N_2O flux densities varied from -19.0 to 105.7 μmol m^{-2} d^{-1} (-14.1–30.3 μmol m^{-2} d^{-1} without the extreme values), with an average of 3.5±12.4 μmol m^{-2} d^{-1} (3.3±6.5 μmol m^{-2} d^{-1} without the extreme values). However, the true emissions might have been underestimated because our monthly sampling resolution is insufficient to capture short-term N_2O accumulation events due to the fast breakdown of stratification in autumn. The uncertainty introduced in the flux density computation was estimated to be 20% (Wanninkhof, 2014). The flux densities at the BE Time-Series Station are comparable to those reported by Bange et al. (1998, 0.4–7.1 μmol m^{-2} d^{-1}) from the coastal waters of the southern Baltic Sea, but are slightly lower than the average N_2O flux density reported by Rönner (1983, 8.9 μmol m^{-2} d^{-1}) from the central Baltic Sea. Please note that the results of Rönner (1983) were obtained only from the summer season and therefore are probably biased because of missing seasonality.

In December 2014, a strong saline water inflow from the North Sea was observed, which was the third strongest ever recorded (Mohrholz et al., 2015). Although the salinity in December 2014 was comparable to other years, a remarkable increase in salinity was observed in the following several months. However, we did not detect a significant N_2O anomaly or enhanced emission during that time. Similarly, Walter et al. (2006) investigated the impact of the North Sea water

inflow on N_2O production in the southern and central Baltic Sea in 2003. The oxygenated water ventilated the deep Baltic Sea and shifted anoxic to oxic condition which led to enhanced N_2O production, but the accumulated N_2O was unlikely to reach the surface due to the presence of a permanent halocline (Walter et al., 2006).

Although we observed extremely high N_2O flux density in November 2017, the low-N_2O-concentration (<10 nM) events have become more and more frequent during the past ten years (Fig. 2). This phenomenon seldom occurred before 2011, but remarkable low N_2O concentrations can be seen in 2011 and 2013, and to a less extent in 2012 and 2014. Similar events lasted for several months in 2015 and for even more than half a year during 2016–2017. The most striking was that the low-N_2O-concentration water was not only detected in bottom waters, but also at surface which would significantly impact the air-sea N_2O flux densities. Although the MKT result did not give a significant trend for the N_2O flux densities, the data presented in Fig. 8 suggest a potential decline of N_2O flux densities from the coastal Baltic Sea, challenging the conventional view that N_2O emissions from coastal waters would most probably increase in the future, which was based on the hypothesis of increasing nutrient loads into coastal waters. Due to an effective reduction of nutrient inputs, the severe eutrophication condition in the Baltic Sea has been alleviated (HELCOM, 2018b), but ongoing deoxygenation points to the fact that it will take a longer time for coastal ecosystems to feedback to reduced nutrient inputs because other environmental changes such as warming may override decreasing eutrophication (Lennartz et al., 2014).

4. Conclusions

The seasonal and inter-annual N_2O variations at the BE Time-Series Station from July 2005 to December 2017 were driven by the prevailing O_2 regime and nutrients availability. We found a pronounced seasonal cycle with low N_2O concentrations (undersaturations) occurring in hypoxic/anoxic bottom waters in autumn and enhanced concentrations (supersaturations) all over the water column in winter/early spring. Significant decreasing trends for N_2O concentrations were found for few months, while most of the year, no significant trend was detectable in the period of 2005–2017. During 2005–2017, no significant trends were present for O_2 and nutrients either, but these parameters all show significant decreasing trends on longer time scales (~60 years) at BE. Our results show the strong coupling of N_2O with O_2 and nutrient concentrations, and suggest similar changes on comparable time scales. Further monitoring of N_2O at BE time series station is thus important to detect changes. Further studies on N_2O production/consumption by nitrification and denitrification and analysis of the characteristic N_2O isotope signature might be very helpful to decipher the potential roles of O_2/nutrients for N_2O cycling.

Temperature plays a modulating role for the N_2O emission at the BE Time-Series Station. Although the hydrographic condition at BE is generally dominated by the inflow of saline North Sea water, this did not affect N_2O production and its emissions to the atmosphere. It seems that

events with extremely low N_2O concentrations and thus reduced N_2O emissions became more frequent in recent years. Our results provide a new perspective onto potential future patterns of N_2O distribution and emissions in coastal areas. Continuous measurement at the BE Time-Series Station with a focus on late autumn would be of great importance for monitoring and understanding the future changes of N_2O concentrations and emissions in the southwestern Baltic Sea.

Data availability

Data are available from the Boknis Eck Database: www.bokniseck.de

Author contribution

X.M., S.T.L. and H.W.B. designed the study and participated in the fieldwork. N_2O measurements and data processing were done by X.M. and S.T.L. X.M. wrote the manuscript with contributions from S.T.L. and H.W.B.

Competing interests

The authors declare that they have no conflict of interest.

Acknowledgments

The authors thank the captain and crew of the RV *Littorina* and *Polarfuchs* as well as the many colleagues and numerous students who helped with the sampling and measurements of the BE time-series through various projects. Special thanks to A. Kock for her help with sampling, measurements and data analysis. The time-series at BE was supported by DWK Meeresforschung (1957–1975), HELCOM (1979–1995), BMBF (1995–1999), the Institut für Meereskunde (1999–2003), IfM-GEOMAR (2004–2011) and GEOMAR (2012–present). The current N_2O measurements at BE are supported by the EU BONUS INTEGRAL project which receives funding from BONUS (Art 185), funded jointly by the EU, the German Federal Ministry of Education and Research, the Swedish Research Council Formas, the Academy of Finland, the Polish National Centre for Research and Development, and the Estonian Research Council. The Boknis Eck Time-Series Station (www.bokniseck.de) is run by the Chemical Oceanography Research Unit of GEOMAR, Helmholtz Centre for Ocean Research Kiel. Data from BE are available from www.bokniseck.de/database-access. The N_2O data presented here have been archived in MEMENTO (the MarinE MethanE and NiTrous Oxide database: https://memento.geomar.de). X. Ma is grateful to the China Scholarship Council for providing financial support (File No. 201306330056) and the EU BONUS INTEGRAL project.

References

Bange, H. W.: Nitrous oxide and methane in European coastal waters, Estuar. Coast. Shelf S., 70, 361–374, https://doi.org/10.1016/j.ecss.2006.05.042, 2006.

Bange, H. W., Dahlke, S., Ramesh, R., Meyer-Reil, L. A., Rapsomanikis, S., and Andreae, M. O.: Seasonal study of methane and nitrous oxide in the coastal waters of the southern Baltic Sea, Estuar. Coast. Shelf S., 47, 807–817, https://doi.org/10.1006/ecss.1998.0397, 1998.

Battaglia, G. and Joos, F.: Marine N_2O emissions from nitrification and denitrification constrained by modern observations and projected in multimillenial global warming simulations, Global Biogeochem. Cy., 32, 92–121, https://doi.org/10.1002/2017GB005671, 2018.

Bonin, P., Gilewicz, M., and Bertrand, J. C.: Effects of oxygen on each step of denitrification on Pseudomonas nautica, Can. J. Microbiol., 35, 1061–1064, https://doi.org/10.1139/m89-177, 1989.

Breitburg, D., Levin, L. A., Oschlies, A., Grégoire, M., Chavez, F. P., Conley, D. J., Garçon, V., Gilbert, D., Gutiérrez, D., Isensee, K., Jacinto, G. S., Limburg, K. E., Montes, I., Naqvi, S. W. A., Pitcher, G. C., Rabalais, N. N., Roman, M. R., Rose, K. A., Seibel, B. A., Telszewski, M., Yasuhara, M., and Zhang, J.: Declining oxygen in the global ocean and coastal waters, Science, 359, eaam7240, http://dx.doi.org/10.1126/science.aam7240, 2018.

Capelle, D. W., Hawley, A. K., Hallam, S. J., and Tortell, P. D.: A multi-year time-series of N_2O dynamics in a seasonally anoxic fjord: Saanich Inlet, British Columbia, Limnol. Oceanogr., 63, 524–539, https://doi.org/10.1002/lno.10645, 2018.

Carstensen, J., Andersen, J. H., Gustafsson, B. G., and Conley, D. J.: Deoxygenation of the Baltic Sea during the last century, P. Natl. Acad. Sci. USA, 111, 5628–5633, https://doi.org/10.1073/pnas.1323156111, 2014.

Codispoti, L. A., Elkins, J. W., Yoshinari, T., Fredrich, G., Sakamoto, C., and Packard, T.: On the nitrous oxide flux from productive regions that contain low oxygen waters, in: Oceanography of the Indian Ocean, edited by Desai, B. N., Oxford Univ. Press, New York, 271–284, 1992.

Codispoti, L. A., Brandes, J. A., Christensen, J. P., Devol, A. H., Naqvi, S. W. A., Paerl, H. W., and Yoshinari, T.: The oceanic fixed nitrogen and nitrous oxide budgets: Moving targets as we enter the anthropocene? Sci. Mar., 65, 85–105, https://doi.org/10.3989/scimar.2001.65s285, 2001.

Codispoti, L. A., Yoshinari, T., and Devol, A. H.: Suboxic respiration in the oceanic water column, in: Respiration in aquatic ecosystems, edited by del Giorgio, P. A. and Williams, P. J., Oxford Univ. Press, New York, 225–247, 2005.

Conley, D. J., Carstensen, J., Aigars, J., Axe, P., Bonsdorff, E., Eremina, T., and Lannegren, C.: Hypoxia is increasing in the coastal zone of the Baltic Sea, Environ. Sci. Technol., 45, 6777–6783, doi: 10.1021/es201212r, 2011.

Cornejo, M., Murillo, A. A., and Farías, L.: An unaccounted for N_2O sink in the surface water of the eastern subtropical South Pacific: Physical versus biological mechanisms, Prog. Oceanogr., 137, 12–23, https://doi.org/10.1016/j.pocean.2014.12.016, 2015.

Dale, A. W., Sommer, S., Bohlen, L., Treude, T., Bertics, V. J., Bange, H. W., Pfannkuche, O., Schorp, T., Mattsdotter, M., and Wallmann, K.: Rates and regulation of nitrogen cycling in seasonally hypoxic sediments during winter (Boknis Eck, SW Baltic Sea): Sensitivity to environmental variables, Estuar. Coast. Shelf S., 95, 14–28, https://doi.org/10.1016/j.ecss.2011.05.016, 2011.

Ducklow, H. W., Doney, S. C., and Steinberg, D. K.: Contributions of long-term research and time-series observations to marine ecology and biogeochemistry, Annu. Rev. Mar. Sci., 1, 279–302, https://doi.org/10.1146/annurev.marine.010908.163801, 2009.

Farías, L., Castro-González, M., Cornejo, M., Charpentier, J., Faúndez, J., Boontanon, N., and Yoshida, N.: Denitrification and nitrous oxide cycling within the upper oxycline of the eastern tropical South Pacific oxygen minimum zone, Limnol. Oceanogr., 54, 132–144, https://doi.org/10.4319/lo.2009.54.1.0132, 2009.

Farías, L., Faúndez, J., Fernández, C., Cornejo, M., Sanhueza, S., and Carrasco, C.: Biological N_2O fixation in the Eastern South Pacific Ocean and marine cyanobacterial cultures, Plos one, 8, e63956, https://doi.org/10.1371/journal.pone.0063956, 2013.

Farías, L., Besoain, V., and García-Loyola, S.: Presence of nitrous oxide hotspots in the coastal upwelling area off central Chile: an analysis of temporal variability based on ten years of a biogeochemical time series, Environ. Res. Lett., 10, 044017, doi:10.1088/1748-9326/10/4/044017, 2015.

Goreau, T. J., Kaplan, W. A., Wofsy, S. C., McElroy, M. B., Valois, F. W., and Watson, S.W.: Production of NO_2^- and N_2O by nitrifying bacteria at reduced concentrations of oxygen, Appl. Environ. Microb., 40, 526–532, 1980.

Grasshoff, K., Kremling, K., and Ehrhardt, M.: Methods of seawater analysis, 3rd edition, WILEY-VCH, Weihheim, Germany, 1999.

Hannig, M., Lavik, G., Kuypers, M. M. M., Woebken, D., Martens-Habbena, W., and Jürgens, K.: Shift from denitrification to anammox after inflow events in the central Baltic Sea, Limnol. Oceanogr., 52, 1336–1345, 2007.

Hansen, H. P., Giesenhagen, H. C., and Behrends, G.: Seasonal and long-term control of bottom water oxygen deficiency in a stratified shallow-coastal system, ICES J. Mar. Sci., 56, 65–71, doi: 10.1006/jmsc.1999.0629, 1999.

HELCOM: Sources and pathways of nutrients to the Baltic Sea, Baltic Sea Environ. Proc., 153, 2018a.

HELCOM: State of the Baltic Sea - Second HELCOM holistic assessment 2011–2016, Baltic Sea Environ. Proc., 155, http://stateofthebalticsea.helcom.fi/, 2018b.

Hietanen, S., and Lukkari, K.: Effects of short-term anoxia on benthic denitrification, nutrient fluxes and phosphorus forms in coastal Baltic sediment, Aquat. Microb. Ecol., 49, 293–302, https://doi.org/10.3354/ame01146, 2007.

Hsu, S. A., Meindl, E. A., and Gilhousen, D. B.: Determining the power-law wind-profile exponent under near-neutral stability conditions at sea, J. Appl. Meteorol., 33, 757–765, https://doi.org/10.1175/1520-0450(1994)033<0757:DTPLWP>2.0.CO;2, 1994.

IPCC: Climate Change 2013: The physical science basis. Contribution of Working Group I to the fifth assessment report of the Intergovernmental Panel on Climate Change, Cambridge University Press, Cambridge, UK and New York, NY, 2013.

Landolfi, A., Somes, C. J., Koeve, W., Zamora, L. M., and Oschlies, A.: Oceanic nitrogen cycling and N_2O flux perturbations in the Anthropocene, Global Biogeochem. Cy., 31, 1236–1255, doi:10.1002/2017GB005633, 2017.

Lennartz, S. T., Lehmann, A., Herrford, J., Malien, F., Hansen, H. P., Biester, H., and Bange, H. W.: Long-term trends at the Boknis Eck time series station (Baltic Sea), 1957–2013: does climate change counteract the decline in eutrophication? Biogeosciences, 11, 6323–6339, https://doi.org/10.5194/bg-11-6323-2014, 2014.

Löscher, C. R., Kock, A., Könneke, M., LaRoche, J., Bange, H. W., and Schmitz, R. A.: Production of oceanic nitrous oxide by ammonia-oxidizing archaea, Biogeosciences. 9, 2419–2429, https://doi.org/10.5194/bg-9-2419-2012, 2012.

Kock, A., Arévalo-Martínez, D. L., Löscher, C. R., and Bange, H. W.: Extreme N_2O accumulation in the coastal oxygen minimum zone off Peru, Biogeosciences. 13, 827–840, doi: 10.5194/bg-13-827-2016, 2016.

Kroeze, C., and Seitzinger, S. P.: Nitrogen inputs to rivers, estuaries and continental shelves and related nitrous oxide emissions in 1990 and 2050: a global model, Nutr. Cycl. Agroecosys., 52, 195–212, 1998.

Kulkarni, A., and Von Storch, H.: Monte Carlo experiments on the effect of serial correlation on the Mann-Kendall test of trend, Meteorol. Z., 4, 82–85, 1995.

Martinez-Rey, J., Bopp, L., Gehlen, M., Tagliabue, A., and Gruber, N.: Projections of oceanic N_2O emissions in the 21st century using the IPSL Earth system model, Biogeosciences, 12, 4133–4148, doi: 10.5194/bg-12-4133-2015, 2015.

Meier, H. M., Väli, G., Naumann, M., Eilola, K., and Frauen, C.: Recently accelerated oxygen consumption rates amplify deoxygenation in the Baltic Sea, J. Geophys. Res.-Oceans., 123, 3227–3240, https://doi.org/10.1029/2017JC013686, 2018.

Mohrholz, V., Naumann, M., Nausch, G., Krüger, S., and Gräwe, U.: Fresh oxygen for the Baltic Sea-An exceptional saline inflow after a decade of stagnation, J. Marine Syst., 148, 152-166, https://doi.org/10.1016/j.jmarsys.2015.03.005, 2015.

Naqvi, S. W. A., Jayakumar, D. A., Narvekar, P. V., Naik, H., Sarma, V. V. S. S., D'souza, W., Joseph, S., and George, M. D.: Increased marine production of N_2O due to intensifying anoxia on the Indian continental shelf, Nature, 408, 346, 2000.

Naqvi, S.W.A., Bange, H.W., Farías, L., Monteiro, P.M.S., Scranton, M.I., and Zhang, J.: Marine hypoxia/anoxia as a source of CH_4 and N_2O, Biogeosciences, 7, 2159–2190, https://doi.org/10.5194/bg-7-2159-2010, 2010.

Nevison, C., Butler, J. H., and Elkins, J. W.: Global distribution of N_2O and the ΔN_2O-AOU yield in the subsurface ocean, Global Biogeochem. Cy., 17, https://doi.org/10.1029/2003GB002068, 2003.

Nightingale, P., G. Malin, C. S. Law, A. J. Watson, P. S. Liss, M. I. Liddicoat, J. Boutin, and R. C. Upstill-Goddard: In situ evaluation of air-sea gas exchange parameterizations using novel conservative and volatile tracers, Global Biogeochem. Cy., 14, 373–387, https://doi.org/10.1029/1999GB900091, 2000.

Rabalais, N. N., Cai, W.-J., Carstensen, J., Conley, D. J., Fry, B., Hu, X., Quinones-Rivera, Z., Rosenberg, R., Slomp, C. P., Turner, R. E., Voss, M., Wissel, B., and Zhang, J.: Eutrophication-driven deoxygenation in the coastal ocean, Oceanography, 27, 172–183, https://doi.org/10.5670/oceanog.2014.21, 2014.

Ravishankara, A. R., Danielm J., S., and Portmann, R. W.: Nitrous oxide (N_2O): the dominant ozone-depleting substance emitted in the 21st century, Science, 326, 123–125, doi: 10.1126/science.1176985, 2009.

Rönner, U.: Distribution, production and consumption of nitrous oxide in the Baltic Sea, Geochim. Cosmochim. Ac., 47, 2179–2188, https://doi.org/10.1016/0016-7037(83)90041-8, 1983.

Schlittgen, R., and Streitberg, B. H. J.: Zeitreihenanalyse, Oldenburg Wissenschaftsverlag, Munich, Germany, 2001.

Seitzinger, S. P., and Kroeze, C.: Global distribution of nitrous oxide production and N inputs in freshwater and coastal marine ecosystems, Global Biogeochem. Cy., 12, 93–113, 1998.

643 Siedler, G., and Peters, H.: Properties of sea water, in: Oceanography, edited by Sündermann J.,
644 Springer, Berlin, Heidelberg, 233–264, 1986.

645 Simone, F.: Mann-Kendall Test, MathWorks,
646 https://ww2.mathworks.cn/matlabcentral/fileexchange/25531-mann-kendall-test, 2009.

647 Sohm, J. A., Webb, E. A., and Capone, D. G.: Emerging patterns of marine nitrogen fixation, Nat.
648 Rev. Microbiol., 9, 499–508, doi: 10.1038/nrmicro2594, 2011.

649 Torrence, C., and Compo, G. P.: A practical guide to wavelet analysis, B. Am. Meteorol. Soc.,
650 79, 61–78, https://doi.org/10.1175/1520-0477(1998)079<0061:APGTWA>2.0.CO;2, 1998.

651 Torrence, C., and Compo, G. P.: Wavelet analysis, http://paos.colorado.edu/research/wavelets/,
652 2004.

653 Voss, M., Emeis, K. C., Hille, S., Neumann, T., and Dippner, J. W.: Nitrogen cycle of the Baltic
654 Sea from an isotopic perspective, Global Biogeochem. Cy., 19, doi: 10.1029/2004GB002338,
655 2005.

656 Walter, S., Breitenbach, U., Bange, H. W., Nausch, G., and Wallace, D. W.: Distribution of N_2O
657 in the Baltic Sea during transition from anoxic to oxic conditions, Biogeosciences, 3, 557–570,
658 https://doi.org/10.5194/bg-3-557-2006, 2006.

659 Wanninkhof, R.: Relationship between wind speed and gas exchange over the ocean revisited,
660 Limnol. Oceanogr.: Methods, 12, 351–362, https://doi.org/10.4319/lom.2014.12.351, 2014.

661 Weiss, R. F., and Price, B. A.: Nitrous oxide solubility in water and seawater, Mar. Chem., 8,
662 347–359, https://doi.org/10.1016/0304-4203(80)90024-9, 1980.

663 Wilson, S. T., Ferrón, S., and Karl, D. M.: Interannual variability of methane and nitrous oxide in
664 the North Pacific Subtropical Gyre, Geophys. Res. Lett., 44, 9885–9892,
665 https://doi.org/10.1002/2017GL074458, 2017.

666 Xu, Z. X., Takeuchi, K., and Ishidaira, H.: Monotonic trend and step changes in Japanese
667 precipitation, J. Hydrol., 279, 144–150, https://doi.org/10.1016/S0022-1694(03)00178-1, 2003.

668 Yang, D., Li, C., Hu, H., Lei, Z., Yang, S., Kusuda, T., Koike, T., and Musiake, K.: Analysis of
669 water resources variability in the Yellow river of China during the last half century using the
670 historical data, Water Resour. Res., 40, 1–12, https://doi.org/10.1029/2003WR002763, 2004.

671 Zhang, G.-L., Zhang, J., Liu, S.-M., Ren, J.-L., and Zhao, Y.-C.: Nitrous oxide in the Changjiang
672 (Yangtze River) estuary and its adjacent marine area: Riverine input, sediment release and
673 atmospheric fluxes, Biogeosciences, 7, 3505–3516, https://doi.org/10.5194/bg-7-3505-2010,
674 2010.

675 Table 1. The results of the Mann-Kendall test for the surface and bottom N_2O concentrations and
676 saturations of the 12 individual months.

677 Table 1a. MKT results for N_2O concentrations

Month	January		February		March		April	
Depth/m	1	25	1	25	1	25	1	25
p	0.09	0.19	0.11	0.03(-)	0.19	0.63	0.09	0.30
Month	May		June		July		August	
Depth/m	1	25	1	25	1	25	1	25
p	0.63	0.24	0.15	0.95	0.16	0.16	0.20	0.03(-)
Month	September		October		November		December	
Depth/m	1	25	1	25	1	25	1	25
p	0.25	0.76	0.36	0.76	0.67	0.16	0.10	0.30

678

679 Table 1b. MKT results for N_2O saturations

Month	January		February		March		April	
Depth/m	1	25	1	25	1	25	1	25
p	0.37	0.24	0.15	0.15	0.19	0.63	0.11	0.19
Month	May		June		July		August	
Depth/m	1	25	1	25	1	25	1	25
p	0.19	1	0.37	0.54	0.10	0.43	0.20	0.02(-)
Month	September		October		November		December	
Depth/m	1	25	1	25	1	25	1	25
p	0.04(-)	0.85	0.06	0.43	0.20	0.03(-)	0.16	0.36

680

681 p indicates the p-value of the test, which is the probability, under the null hypothesis, of obtaining a value of
682 the test statistic as extreme or more extreme than the value computed from the sample.
683 (-) indicates a rejection of the null hypothesis at α significance level and a decreasing trend is detected.

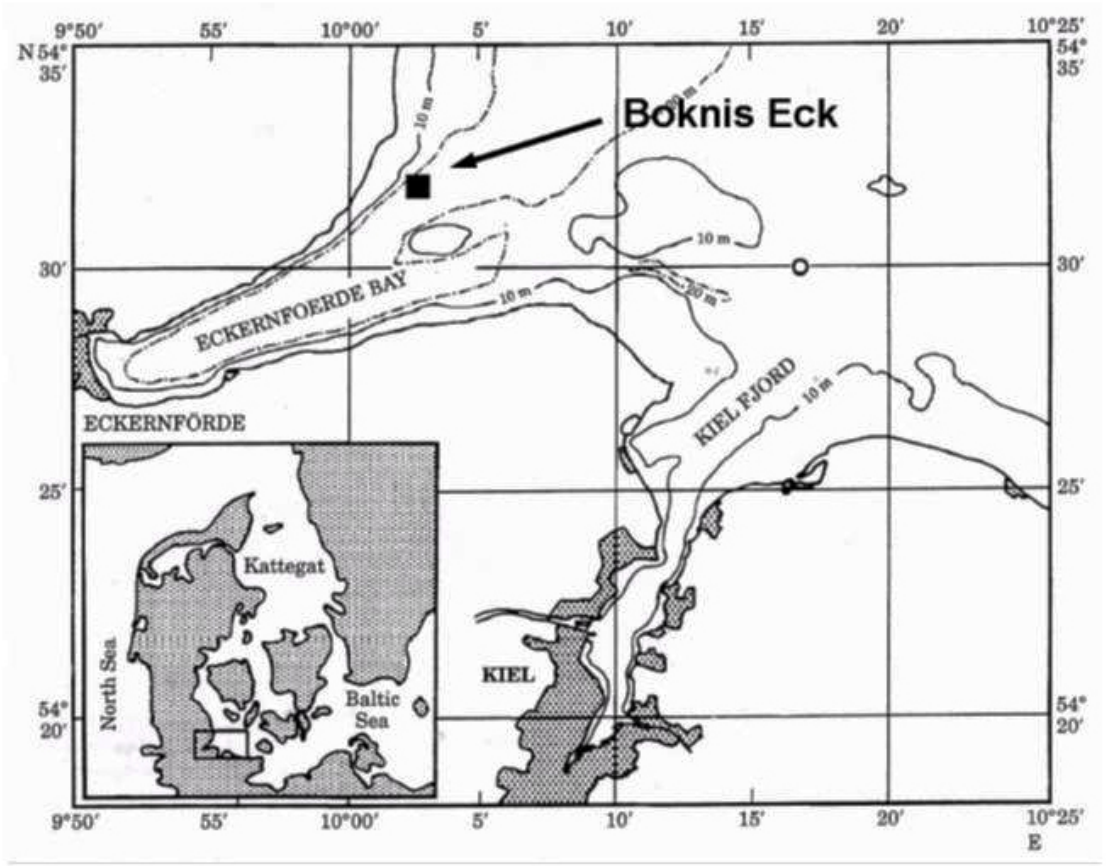

684

685 Fig. 1 Location of the Boknis Eck Time-Series Station in the Eckernförde Bay, southwestern Baltic Sea. (Map
686 from Hansen et al., 1999)

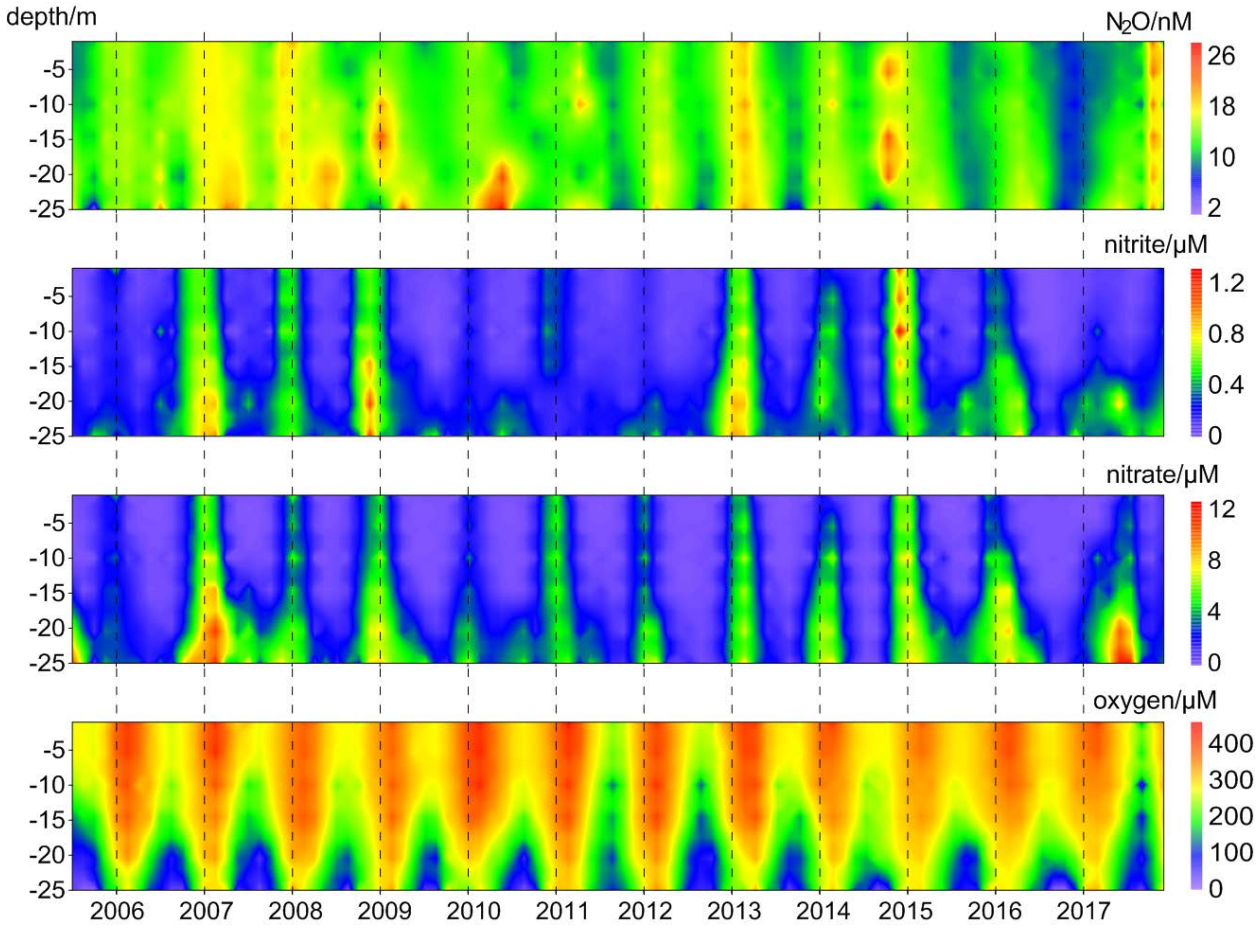

687

688 Fig. 2 Vertical distributions of dissolved O_2, NO_2^-, NO_3^-, and N_2O from the BE Time-Series Station during
689 2005–2017.

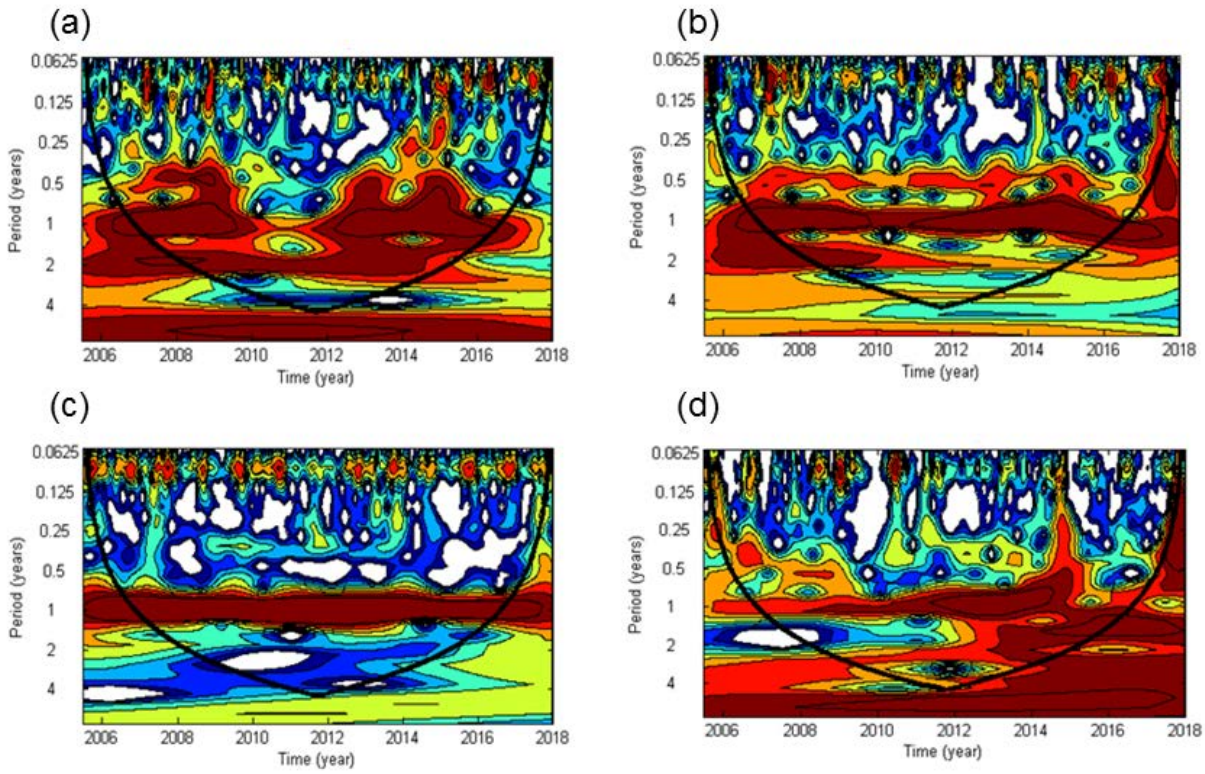

690

691 Fig. 3 Wavelet power spectra of NO_2^- (a), NO_3^- (b), dissolved O_2 (c) and N_2O (d) from the BE Time-Series
692 Station. Red areas indicate high, blue indicate low power. The black conic line indicates the significant area
693 where boundary effects can be excluded.

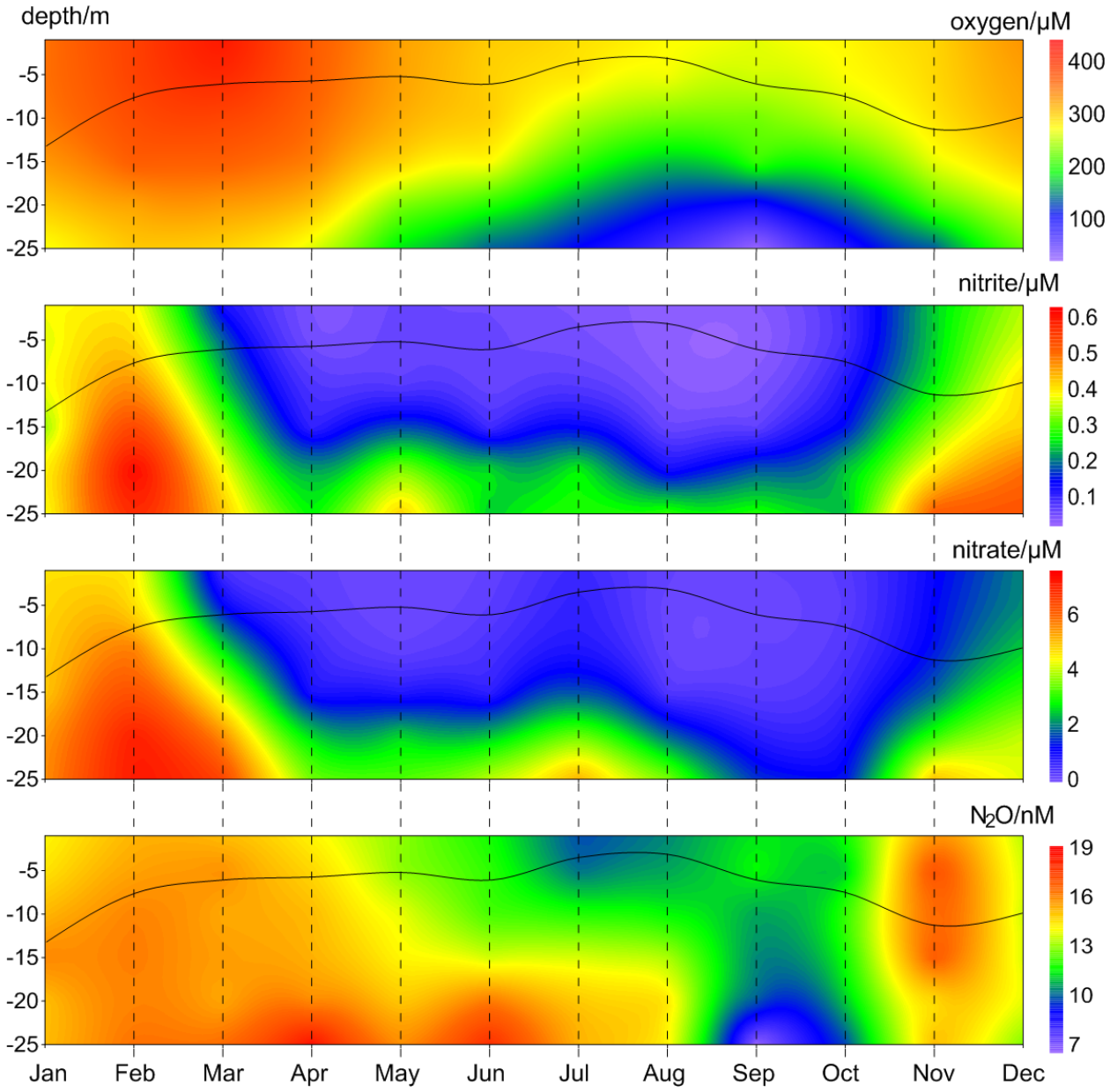

Fig. 4 Average vertical distributions of dissolved O_2, NO_2^-, NO_3^-, and N_2O from the BE Time-Series Station during 2005–2017. The black line indicates the mixed layer depth, which was calculated based on a potential density anomaly of 0.15 kg m^{-3} from the sea surface (1m).

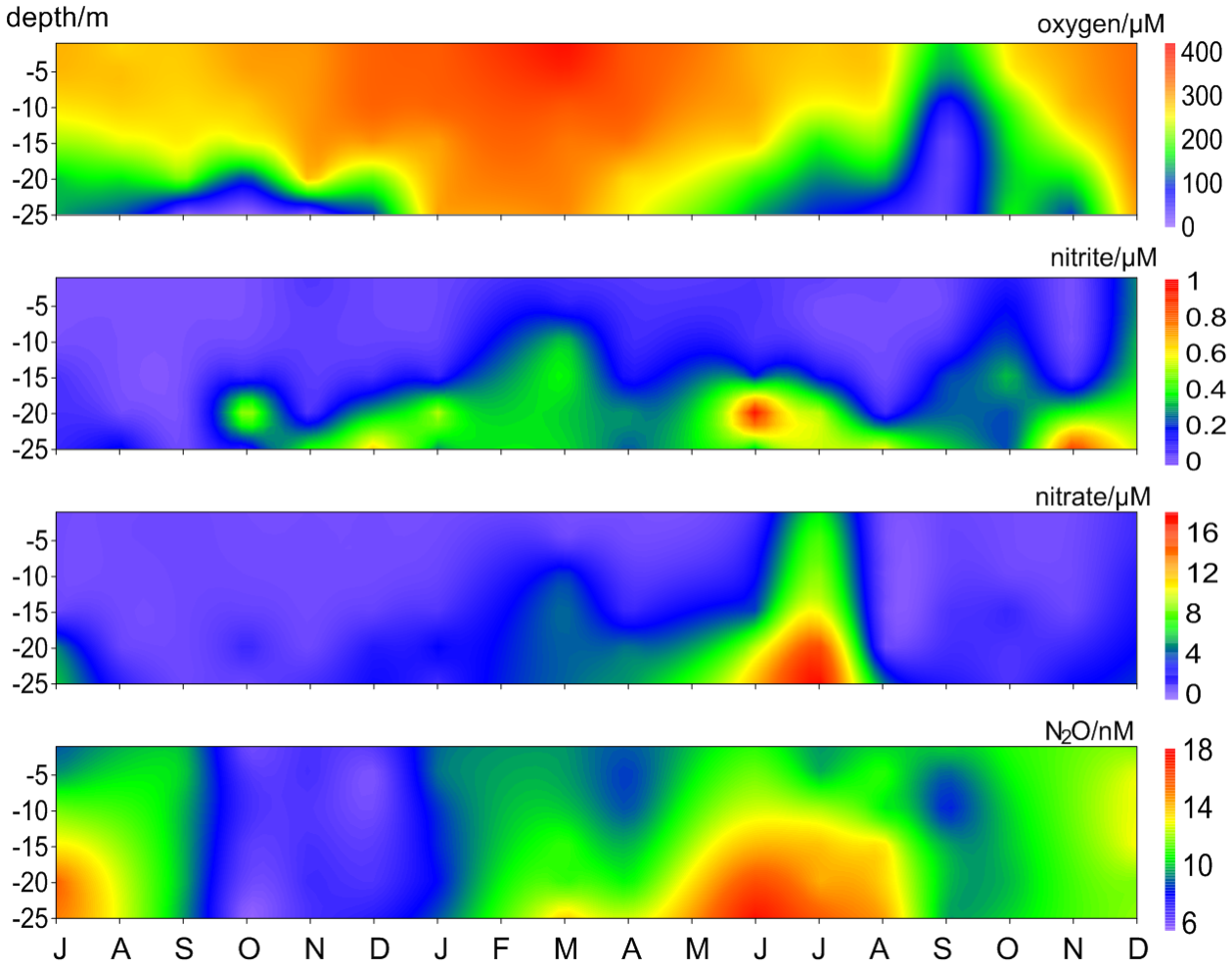

Fig. 5 Vertical distribution of dissolved O_2, NO_2^-, NO_3^-, and N_2O from the BE Time-Series Station during July 2016–December 2017. Please note that the high N_2O concentrations in November 2017 were removed for better visualization.

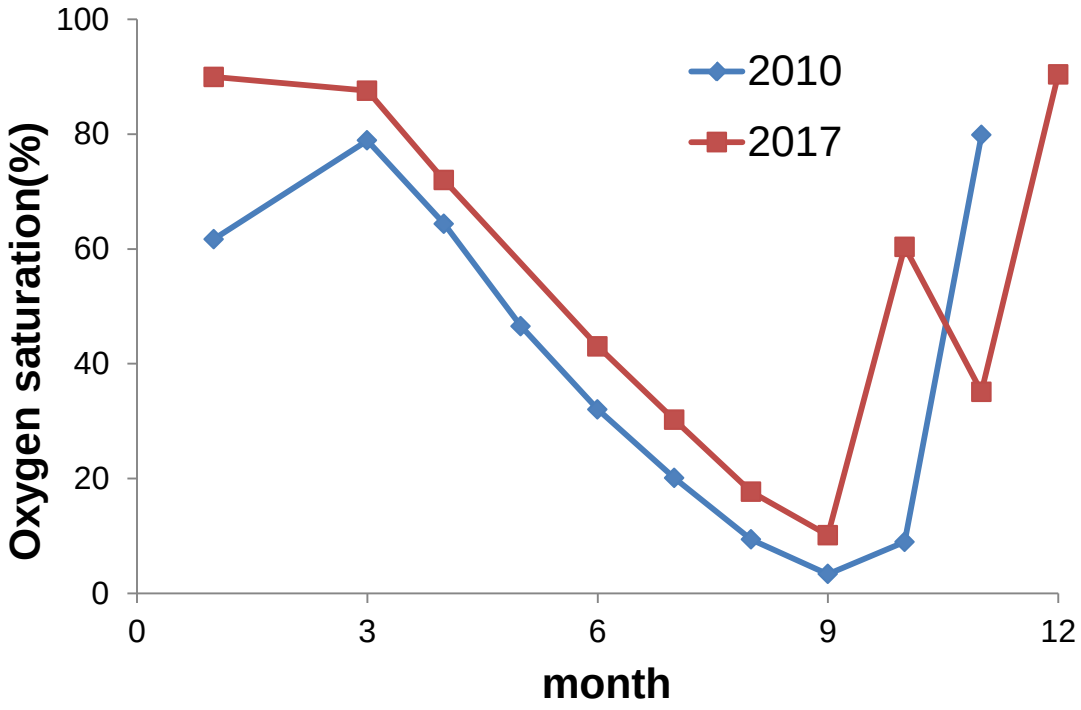

Fig. 6 Variations of bottom O_2 saturation in 2010 (blue) and 2017 (red).

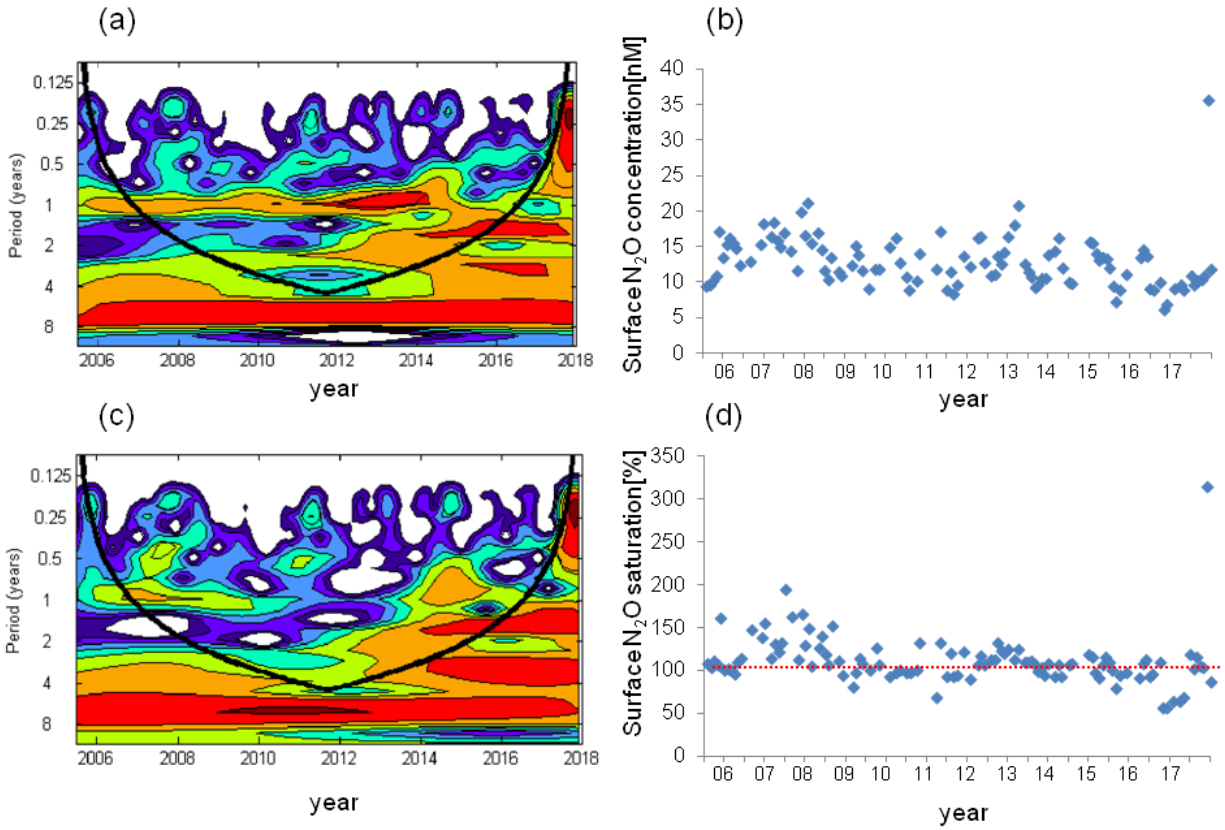

704

705 Fig. 7 Wavelet analysis and the variation of surface N_2O concentrations (a, b) and surface N_2O saturations (c,
706 d). The dashed red line in (d) indicates the saturation of 100%.

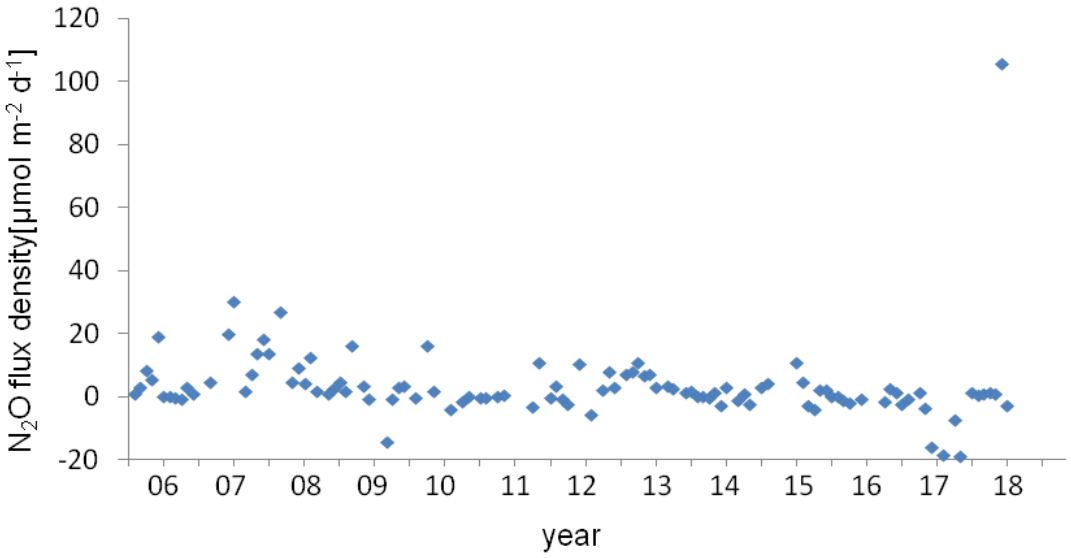

Fig. 8 Variation of N_2O flux density at the BE Time Series-Station during 2005–2017. Negative values indicated N_2O influx from the atmosphere and positive values indicated N_2O efflux to the atmosphere.